Genome-wide circadian rhythm detection methods: systematic evaluations and practical guidelines

Wenwen Mei[1,*], Zhiwen Jiang[1,*], Yang Chen[2], Li Chen[3], Aziz Sancar[4,5,#], Yuchao Jiang[1,5,6,#]

[1] Department of Biostatistics, Gillings School of Global Public Health, University of North Carolina, Chapel Hill, NC 27599, USA.

[2] Department of Statistics and Michigan Institute for Data Science, University of Michigan, Ann Arbor, MI 48109, USA.

[3] Department of Medicine and Center for Computational Biology and Bioinformatics, Indiana University School of Medicine, Indianapolis, IN 46202, USA.

[4] Department of Biochemistry and Biophysics, School of Medicine, University of North Carolina, Chapel Hill, NC 27599, USA.

[5] Lineberger Comprehensive Cancer Center, University of North Carolina, Chapel Hill, NC 27599, USA.

[6] Department of Genetics, School of Medicine, University of North Carolina, Chapel Hill, NC 27599, USA.

Wenwen Mei is a PhD student in the Department of Biostatistics at the University of North Carolina at Chapel Hill.

Zhiwen Jiang is a MS student in the Department of Biostatistics at the University of North Carolina at Chapel Hill.

Yang Chen is an Assistant Professor in the Department of Statistics and Research Assistant Professor at the Michigan Institute of Data Science at the University of Michigan.

Li Chen is an Assistant Professor in the Dpartment of Medicine and a member of the Center for Computational Biology and Bioinformatics at Indianna University School of Medicine.

Aziz Sancar is the Sarah Graham Kenan Professor of Biochemistry and Biophysics at the University of North Carolina School of Medicine and member of UNC Lineberger Comprehensive Cancer Center.

Yuchao Jiang is an Assistant Professor in the Department of Biostatisrtics and the Department of Genetics at Univerity of North Carolina at Chapel Hill and member of UNC Lineberger Comprehensive Cancer Center.

∗ These authors contributed equally.

To whom correspondence should be addressed. Email: aziz_sancar@med.unc.edu; yuchaoj@email.unc.edu.

ABSTRACT

Circadian rhythms are oscillations of behavior, physiology, and metabolism in many organisms. Recent advancements in omics technology make it possible for genome-wide profiling of circadian rhythms. Here, we conducted a comprehensive analysis of seven existing algorithms commonly used for circadian rhythm detection. Using gold-standard circadian and non-circadian genes, we systematically evaluated the accuracy and reproducibility of the algorithms on empirical datasets generated from various omics platforms under different experimental designs. We also carried out extensive simulation studies to test each algorithm's robustness to key variables, including sampling patterns, replicates, waveforms, signal-to-noise ratios, uneven samplings, and missing values. Furthermore, we examined the distributions of the nominal p-values under the null and raised issues with multiple testing corrections using traditional approaches. With our assessment, we provide method selection guidelines for circadian rhythm detection, which are applicable to different types of high-throughput omics data.

Key words: biological rhythm; circadian rhythm detection; benchmarking; omics; precision and recall; reproducibility.

Key points

- Various methods have been developed for circadian rhythm detection on a genome-wide scale using omics technologies, yet there has not been a comprehensive summary and evaluation of all existing methods to date.
- Using gold-standard circadian and non-circadian genes, we systematically evaluated the accuracy and reproducibility of seven existing algorithms for circadian rhythm detection on empirical datasets generated from various omics platforms.
- We carried out extensive simulation studies to test each algorithm's robustness to key variables, including sampling patterns, replicates, waveforms, signal-to-noise ratios, uneven samplings, and missing values.
- We examined the distributions of the nominal *p*-values under the null and raised issues with multiple testing corrections using the Benjamini-Hochberg procedure due to gene-gene correlation and testing being overly conservative.
- We provide method selection guidelines for circadian rhythm detection, which are applicable to different types of high-throughput omics data.

BACKGROUND

Circadian rhythms are approximately 24-hour oscillations of behavior, physiology, and metabolism that exist in almost all living organisms ranging from prokaryotes to mammals [1, 2]. Circadian rhythm is regulated by the circadian system, which consists of many "clock-controlled genes" that exhibit oscillatory patterns [1]. These oscillations provide organisms with an adaptive advantage by enabling them to predict and adjust to the variations within their environments [3]. Additionally, and perhaps more importantly, disruptions of circadian rhythms have shown to contribute to numerous diseases, including metabolic disorders, heart disease, and aging [4-7]. It is, therefore, of great importance and interest to perform genome-scale analysis of biological rhythms.

Recent advances in omics technologies, including both microarrays and next-generation sequencing, offer appealing platforms to identify circadian genes on a genome-wide scale. These have, indeed, led to the proposal of multifarious methodologies adopted from various fields including mathematics, statistics, astrophysics, etc. The earliest of the selected methods is Lomb-Scargle (LS) periodogram [8], an algorithm adapted from astrophysics that detects oscillations by comparing the data to sinusoidal reference curves of varying periods and phases [9, 10]. ARSER is an algorithm that employs autoregressive spectral estimation to predict periodicity and applies a harmonic regression model to fit the time-series [11]. Unlike the model-based LS and ARSER, JTK_CYCLE is a non-parametric method that detects oscillations by comparing the ranks of the measured values to a set of prespecified symmetric reference curves [3]. Both RAIN and eJTK_CYCLE build on the strengths of JTK_CYCLE: RAIN includes an additional set of asymmetric waveforms and examines the increasing and decreasing portions of the curve separately [12]; eJTK_CYCLE improves JTK_CYCLE by explicitly calculating the null distribution such that it accounts for multiple hypothesis testing and by including non-sinusoidal reference waveforms [13]. Based on the successes of the aforementioned methods, MetaCycle proposes an ensemble framework that integrates results from three different algorithms, LS, ARSER, and JTK_CYCLE [14]. Specifically, MetaCycle detects periodicity using the best of breed methods: its p-values are generated using Fisher's method; its periods and phase estimations are integrated using arithmetic and circular means; and a new periodic model, formulated from ordinary least squares

method, is applied to recalculate the amplitude. The most recent method, BIO_CYCLE, is a deep neural network trained on both simulated and empirical circadian and noncircadian time-series [15]. More general information and characteristics of each method are summarized in Table 1.

Multiple studies [10, 16, 17] have evaluated the performance of different methods for circadian rhythm detection, showing discrepancies among the methods, whose performances depend on multiple factors including experimental designs, waveforms of interest, etc. However, there has not been, to our best knowledge, a comprehensive summary and evaluation of all existing methods to date. Here, we systematically assess the performance of the seven aforementioned algorithms for circadian rhythm detection: LS, ARSER, JTK_CYCLE, RAIN, eJTK_CYCLE, MetaCycle, and BIO_CYCLE.

Specifically, we demonstrated and benchmarked the algorithms using real datasets with gold-standard circadian and non-circadian genes. All empirical data were generated using the liver tissue from *Mus musculus* that had undergone two different experimental designs. Under the dark-dark experimental design (24-hour darkness), we focused on using data from gene expression microarrays to assess the accuracy and reproducibility of each algorithm; under the light-dark experimental design (12-hour light followed by 12-hour darkness), we adopted four different next-generation sequencing platforms and explored the robustness of each method in identifying circadian genes. Furthermore, to extend our assessment to non-transcriptomic datasets, we included a proteomic dataset in our evaluation. In addition, we carried out extensive simulation studies to study how key variables, including sampling patterns, replicates, waveforms, signal-to-noise ratios, uneven samplings, missing values, affect the performance of each method. Lastly, we point out the flaw with using the Benjamini-Hochberg procedure to control for false discovery rate. Through these, we offer guidelines on experimental designs as well as best practices and methods of choice to increase the rigor and reproducibility in the analysis of large-scale circadian rhythms. To assist with the comparison of future methods and datasets using our framework, we provide detailed vignettes on applications of existing methods and performance evaluations with source code available at https://github.com/wenwenm183/Circadian_Genes_Benchmark.

RESULTS

Performance assessment using empirical datasets with dark-dark design

We first adopted three gene expression microarray datasets from Hughes et al. [18], Hughes et al. [19], and Zhang et al. [20]. For all three studies, mouse liver samples were collected in every hour or every two-hour under the dark-dark experimental design for 48 hours. We named these three datasets after the first author's last name and the year of publication as Hughes 2009, Hughes 2012, and Zhang 2014, respectively. In addition, we generated a new downsampled dataset from the Hughes 2009 dataset by keeping the even time-points only, and named it “Downsampled Hughes 2009”. Refer to Table 2A for details of the data. Figure 1 shows the scaled gene expression levels of four known circadian and four non-circadian genes. The circadian genes, including the well-studied *Clock*, *Cry1*, *Npas2*, and *Per1* [10], show oscillatory patterns that can be well reproduced across studies, while the non-circadian genes exhibit only noisy signals.

We set out to apply the seven algorithms to these four datasets to detect significantly cyclic genes and evaluate their performances using 104 circadian [10] and 113 non-circadian genes [21] from previous studies (Supplementary Table 1). The accuracy of each method in Hughes 2009, Downsampled Hughes 2009, Hughes 2012, and Zhang 2014 was first assayed with the precision and recall rates for each algorithm given three p-value thresholds, 0.000005 (Bonferroni), 0.00005, 0.0005, and one q-value threshold 0.05 (Benjamini-Hochberg). Due to the tradeoff between sensitivity and specificity, with more relaxed thresholds of significance, the precision rates of all methods decrease while the recall rates increase – the 0.05 q-value threshold achieves the lowest precision rate yet the highest recall rate for any given method (Figure 2A). While there does not exist a single method that consistently achieves the highest precision or recall rate, JTK_CYCLE and BIO_CYCLE are more effective in controlling for false positives while still detecting true circadian genes. For the other methods, however, there is a much higher variability in precision, especially in the Zhang 2014 dataset (Figure 2A). RAIN and MetaCycle tend to have the highest sensitivity/recall, but this can come with significant sacrifice on precision (Figure 2A).

In addition, we find that higher sampling frequency can significantly improve the recall rates of all methods. While MetaCycle and RAIN achieve the apparently higher

recall rate under different thresholds in dataset sampled at a lower frequency (2 h/2 days), all methods, except for LS, produce comparable recall rates when applied to the Hughes 2009 dataset, which is sampled at 1 h/2 days (Figure 2A). Notably, when analyzing the three datasets with lower sampling frequencies, LS failed under all circumstances with recall rates less than 0.1 (Figure 2A). This is due to the extreme p-value distribution of the method with a spike at one, which we will discuss in more detail under "Correlated multiple testing and non-uniform distribution of p-values under the null".

We further computed with the receiver operating characteristic (ROC) curves with a varying threshold on the nominal p-values returned by each method (Figure 2B). The area under the curve (AUC) values serve as a joint measure of sensitivity and specificity and are above 0.80 across all benchmark results, suggesting that all methods achieve good sensitivities while controlling for false positive rates. BIO_CYCLE, the deep-learning-based method, achieves the best performance with the highest AUC across all datasets (Figure 2B).

Reproducibility assessment using empirical datasets with dark-dark design

Reproducibility is one of the core principles for any bioinformatic tools and yet it remains a challenge in the field of circadian rhythm detection, which has not been fully explored. To evaluate the reproducibility of the methods, we first compared and contrasted the significantly cyclic genes returned by each method across the four datasets. To make the input dimensions compatible, we selected a total of 7,570 common genes that are shared across datasets and adopted a q-value threshold of 0.05 for significance. The Venn diagrams in Figure 3A show the overlapping relationships of the significant genes returned by each method. While the experimental designs are the same and the observed gene expression measurements are highly concordant (Figure 1), significant discrepancies of the calling results are observed. Of the seven benchmarked methods, ARSER resulted in 721 overlapping significant genes, which is the highest. This is followed by RAIN, eJTK_CYCLE, MetaCycle, BIO_CYCLE, JTK_CYCLE, and LS with 613, 528, 485, 296, 204, and 0 mutually identified positives, respectively. As mentioned previously, LS failed in detecting any significant oscillations for three out of the four datasets.

158 To further assess the reproducibility of the methods, we computed the Jaccard
159 index and the Sorensen index to measure the similarities among the results from each
160 method. Details of these metrics are included in the Materials and Methods section. As a
161 result, RAIN achieves one of the highest Jaccard indices for any pair of comparisons and
162 ARSER achieves the highest overall Sorensen index across all datasets (Figure 3B). On
163 the other hand, our results indicate that JTK_CYCLE, eJTK_CYLE, and BIO_CYCLE
164 produce the lowest similarity metrics across all comparisons (Figure 3B).
165
166 **Performance assessment using empirical datasets with light-dark design**
167 Next, we adopted four datasets that underwent light-dark experimental design using
168 different next-generation sequencing platforms (i.e., RNA-seq [22], Nascent-seq [22],
169 GRO-seq [23], and XR-seq [24]) and named each one after its sequencing protocol (Table
170 2B). The four datasets have much fewer numbers of time-points compared to the datasets
171 from the dark-dark design, yet three of the four datasets have technical replicates (Table
172 2B). More details of the data can be found in the Materials and Methods section. The
173 oscillatory patterns of known circadian genes are apparent and similar among the various
174 sequencing technologies (Figure 4A), indicating good data quality.
175 ARSER, despite its high reproducibility, cannot handle replicates, and previous
176 studies have shown that data should never be concatenated [17]. Therefore, we focused
177 on assessing the performance of the other six methods. We first examined the distribution
178 of the nominal p-values of the 104 gold-standard circadian genes returned by each
179 method, visualized as beehive plots in Figure 4B, where LS is significantly underpowered
180 in the detection of circadian genes compared to the other methods, given any of the
181 sequencing platforms. This result can be attributed to LS's inability to effectively detect
182 circadian rhythms in datasets with low sampling resolution, which is concordant with our
183 previous results. We observe that JTK_CYCLE, RAIN, eJTK_CYCLE, MetaCycle, and
184 BIO_CYCLE can withstand the sparse sampling and result in overall good performance.
185 To further assess the performance of the methods, we examined the number of
186 significant genes identified by each method with a false discovery rate (FDR) of 0.05. Of
187 the 9,481 mutual genes in the four datasets, LS did not identify any significant genes in
188 any of the datasets. This result aligns with the results from the previous analysis, where

189 we observed LS as being underpowered. JTK_CYCLE and MetaCycle detected a
190 relatively small number of significant genes by RNA-seq and XR-seq. eJTK_CYCLE
191 identified 2,623 significant genes by RNA-seq, and RAIN and BIO_CYCLE identified
192 2,262 and 1,970 significant genes by XR-seq, respectively. When comparing across
193 different sequencing platforms, we observe that the number of detected significant genes
194 from RNA-seq and XR-seq data is much higher than that of the GRO-seq and Nascent-
195 seq data. This implicates a potential deficiency in detecting gene expression rhythmicity
196 by measuring nascent transcripts.
197 With the identified significant genes, we further carried out a gene set enrichment
198 analysis using the DAVID web server [25, 26] with the default options. Results from the
199 KEGG pathway enrichment analysis are shown in Supplementary Table 2. We find that
200 circadian rhythm is significantly enriched by various algorithms, which are marked with
201 asterisks in Figure 4B. Specifically, we find that of the five methods that were able to
202 identify statistically significant genes from RNA-seq data, all have enriched circadian
203 rhythm pathway. Circadian rhythm is also enriched in the three lists of genes that were
204 identified by eJTK_CYCLE and RAIN as well as two of the three lists of genes identified
205 by BIO_CYCLE.
206
207 **Performance assessment using empirical proteomic dataset of dark-dark design**
208 To assess performance of the various methods on non-transcriptomic data, we adopted
209 a proteomic dataset of mouse livers under dark-dark experimental design from Robles et.
210 al [27]. Refer to the Materials and Methods section for details. Since this dataset consists
211 of replicates and missing values, only LS, JTK_CYCLE, RAIN, and MetaCycle were
212 directly applicable. eJTK_CYCLE was not included due to its inefficiency in handling
213 random missing values across different genes/proteins. We calculated the number of
214 significant proteins identified by each method using an FDR threshold of 0.05
215 (Supplementary Figure 1A). LS identified the least number of oscillatory proteins.
216 JTK_CYCLE and MetaCycle returned a moderate number of significant proteins. RAIN
217 identified the largest number of oscillatory proteins, 582, exceeding that of other methods
218 by more than 300. Heatmaps of scaled measurements of oscillatory proteins identified by
219 at least two methods are shown in Supplementary Figure 1B, where the proteins are

220 ordered based on their inferred phases. With the identified oscillatory proteins, we
221 conducted a gene set enrichment analysis using the DAVID web server. While the results
222 did not indicate that circadian rhythm was significantly enriched by any of the algorithms,
223 KEGG metabolic pathways were significantly enriched by all algorithms but LS
224 (Supplementary Table 3).
225
226 **Performance assessment using synthetic datasets**
227 To provide guidelines for method selection, we evaluated the performance of the seven
228 methods in detecting circadian rhythm by simulations with known ground truths.
229 Examples of waveforms generated for the simulated datasets are shown in
230 Supplementary Table 4. We generated six groups of simulated datasets to investigate
231 how key factors affect the performance, including sampling patterns, replicates,
232 waveforms, signal-to-noise ratios (SNRs), uneven samplings, and missing values.
233 Supplementary Table 5 outlines the six groups of simulations and we leave the detailed
234 setup in the Materials and Methods section. Within each simulation group, we repeated
235 each assessment with three different sampling frequencies to determine whether
236 increasing sampling frequency may have an effect on the aforementioned factors. The
237 three sampling frequencies include 4 h/1 day (six time-points), 3 h/1 day (eight time-
238 points), and 2 h/1 day (twelve time-points) and the results are shown in Figure 5A, 5B,
239 and 5C, respectively.
240 ***Sampling patterns***
241 To determine whether increasing the sampling frequency or lengthening the time-window
242 is more important for each method, we first evaluated the results under the sampling
243 pattern of 4 h/1 day versus 8 h/2 days, 3 h/1 day versus 6 h/2 days, and 2 h/1 day versus
244 4 h/2 days. We did not find strikingly different results within each pair of comparison,
245 indicating that when the total number of data points are fixed, having a denser sampling
246 density and enlarging the sampling time-window tend to have similar impact on
247 performance. However, when we increase the number of data points, the performances
248 of all methods are improved, which is concordant with existing studies [16, 17].
249 BIO_CYCLE generally outperforms the other methods, especially in datasets with lower

250 sampling frequency and shorter time-window, while JTK_CYCLE is the most sensitive to
251 fewer observations.

252 ***Replicates***

253 To investigate the trade-off between replicates and sampling frequency, we compared
254 the results of higher sampling frequency without replicates to those of lower sampling
255 frequency with replicates. We first compared the dataset sampled at 4 h /1 day X1 to the
256 dataset sampled at 8 h/1 day X2. LS, JTK_CYCLE, RAIN, eJTK_CYCLE, and MetaCycle
257 show better performance with replicates, while BIO_CYCLE performs significantly better
258 on densely sampled datasets without replicates. Similar results are seen when we applied
259 the methods to the dataset at 3 h/1 day without replicates and the dataset at 6 h/1 day
260 with replicates. As expected, further increasing the sampling resolution offsets the
261 existing preferences that the methods have for inclusion of replicates or higher sampling
262 density.

263 ***Waveforms***

264 Supplementary Table 4 outlines the different types of periodic waveforms that we
265 generated *in silico* in three broad categories: stationary, non-stationary, and asymmetric
266 ones. Through our simulations, we find that all of the algorithms perform the best in
267 detecting non-stationary waveforms. Additionally, all methods, with the exception of
268 eJTK_CYCLE, perform better on stationary waveforms, compared to asymmetric
269 waveforms. eJTK_CYCLE and RAIN are the top two methods for identifying asymmetric
270 waveforms, which are expected due to their design. This is followed by LS, BIO_CYCLE,
271 MetaCycle, and ARSER. JTK_CYCLE is the least effective in identifying asymmetric
272 waveforms regardless of sampling frequency.

273 ***Signal-to-noise ratios (SNRs)***

274 To test the effects of different noise levels on method performance, we generated various
275 datasets with signal-to-noise ratios of 3, 2, 1, and 0.5. For all methods, our results suggest
276 that the larger the SNRs, the higher the accuracy, as expected. LS, MetaCycle, and
277 BIO_CYCLE are overall the most robust to noises regardless of sampling frequency,
278 while JTK_CYCLE has the poorest performance given high noise levels.

279 ***Uneven samplings***

280 To understand how well the methods deal with uneven samplings, we focus on the results
281 of datasets with one or more uneven time-points. Our results suggest that BIO_CYCLE
282 and LS/MetaCycle outperform the other two compatible methods. Under a sparse
283 sampling design, RAIN and eJTK_CYCLE suffer significantly from an increasing number
284 of uneven samplings; a dense sampling design, on the other hand, rescues the
285 aforementioned methods.

286 ***Missing values***

287 We generated datasets that contain 1%, 5%, and 10% missing data, and benchmarked
288 the four methods that allow missing values. The performances of eJTK_CYCLE and RAIN
289 degrade with an increasing proportion of missing values, while the performances of LS,
290 JTK_CYCLE, and MetaCycle are comparably invariant, especially under dense sampling
291 design. We note that eJTK_CYCLE does not handle missing values efficiently, unless the
292 same sampling time points are missing across all genes, which reduces to uneven
293 sampling. When there is not a shared missing pattern across different genes, the dataset
294 needs to be split into multiple uneven sampling cases, and eJTK_CYCLE needs to be
295 applied separately, followed by results integration. Note that BIO_CYCLE can be applied
296 to datasets with missing values only if there are replicates and the missingness only
297 pertains to part of the replicates. We therefore did not include it in the benchmark.

298 ***Computational efficiency***

299 Last but not least, we evaluated the computational efficiency across all benchmarked
300 methods. For dataset with low sampling resolution, the execution times among the
301 methods are approximately the same (Supplementary Table 6). However, when analyzing
302 data of larger sizes, RAIN requires significantly more time compared to the other methods.
303 The running time for LS, ARSER, and BIO_CYCLE does not change much with varying
304 sampling frequency. The running time for MetaCycle, which integrates results from LS,
305 JTK_CYCLE, and ARSER, is calculated as the total running time of the three methods.

306

307 **Correlated multiple testing and non-uniform distribution of p-values under the null**

308 To detect circadian rhythm across thousands of genes, multiple hypothesis testing
309 corrections are needed [28]. A common FDR threshold of 0.05 is recommended by most

methods and adjusted p-values (q-values) are returned by all methods except for RAIN. In the previous sections, we adopted both Bonferroni and Benjamini-Hochberg procedures for corrections. Here, we more carefully examine such procedures and point out a potential drawback resulted from both correlated multiple testing and non-uniform distributions of the nominal p-values under the null. We started with the observed expression measurements from the Hughes 2009 dataset and generated a "null" dataset by randomly permuting the time labels for each gene (Figure 6A). Such permutations not only deplete each gene's rhythmic signals but also disrupts any gene-gene correlations as observed in the raw data, which are high between genes in the same pathways (Figure 6B). As such, all genes upon permutations are under the true null and additionally all gene-level testing is independent.

Figure 6C shows the distributions of nominal p-values for each method when applied to the dataset before and after permutation. The "U-shaped" histograms of the p-values for LS, JTK_CYCLE, MetaCycle, and RAIN using the original data indicate that there is dependence among the variables in the data. This violates the underlying assumption of uniformity and raises a red flag for using Bonferroni or FDR for error control [28]. A few methods have been developed for p-value adjustment when the tests are correlated [29-31] and such issue has been specifically pointed out by Hutchison and Dinner [32] for circadian rhythm detection.

We further applied the methods to the permuted data without gene-gene correlations. The hypothesis testing by LS, JTK_CYCLE, RAIN, and MetaCycle are still overly conservative, while the testing procedures for ARSER and BIO_CYCLE are biased with an overabundance of p-values around 0.3 and 0.1, respectively. eJTK_CYCLE empirically calculates the null distribution of the p-values via permutations and its enhanced version, booteJTK, speeds up this calculation by approximating the null distribution of the Kendall's tau using a Gamma distribution [33]. This indeed leads to a p-value distribution closest to the null. However, neither eJTK_CYCLE nor booteJTK handles missing values efficiently, as explained previously. As a summary, there is still room for method development to yield p-values that better match the underlying assumption of a uniformly distributed p-values under the null.

341 **DISCUSSION**

342 Here, we propose a benchmark framework to systematically evaluate the performance of
343 seven circadian rhythm detection methods, using high-throughput omics data. The
344 empirical datasets that we adopted in this paper were from microarray [18-20] and RNA-
345 seq [22] to measure gene expression, Nascent-seq [22] and GRO-seq [23] to measure
346 nascent RNA, and XR-seq [24] to measure transcription-coupled repair. While these
347 omics data were generated from different platforms, they focus on directly or indirectly
348 profiling transcription. It has been well studied that biological rhythm goes beyond the
349 transcriptomic transcript-level oscillations [34]. For example, post-translational protein
350 acetylation has been linked to circadian rhythm via mass spectrometry [35, 36]. Moreover,
351 it has been shown that a large number of metabolites and proteins exhibit circadian
352 oscillations [27, 37, 38]. The methods and the evaluation procedures are not limited to
353 transcriptomic studies, but can also be applied to acetylomic, metabolomic, and proteomic
354 experiments.

355 Given the assessment results from both simulations and empirical dataset anaylsis,
356 as well as literature review of the seven methods, we have summarized the strengths and
357 weaknesses of each method in Table 3. In general, LS, RAIN, eJTK_CYCLE, and
358 MetaCycle are more versatile in that they can be applied to datasets with replicates,
359 uneven samplings, or missing values. eJTK_CYCLE and BIO_CYCLE generally
360 outperform the other methods under most situations except for handling missing values.
361 On the other hand, JTK is sensitive to high noise levels and low sampling resolutions,
362 and LS cannot detect any significant genes when sampling resolution is lower than 2 h/2
363 days with an FDR threshold of 0.05. The best detection algorithm depends on
364 experimental designs and characteristics of the input data. Therefore, we have created
365 two decision trees, one for low sampling resolution and the other for high sampling
366 resolution, that outline the recommended method(s) under different scenarios
367 (Supplementary Figure 2).

368 Recent advances of high-throughput technologies enable circadian rhythm
369 detection on the genome-wide scale. As with all genomic data, the multi-time-point omics
370 data for circadian rhythm detection bear both technical and biological variability, which
371 can bias the analysis if not properly accounted. Data normalization and batch effect

correction are crucial to remove technical biases and artifacts [39]. Cross-subject variability in rhythmic profiles, especially for human subjects, is a non-negligible source of genetic variation that needs to be adjusted [14]. This is especially important in the case-control setting where multiple subjects are involved. While we did not particularly focus on differential analysis since it is outside the scope of this paper, a few methods, including LimoRhyde [40] and DODR [12] have been made available for differential rhythmicity analysis under different conditions.

Increasingly more circadian omics data are being made available through existing studies and databases [34, 41]. We showed, from our empirical studies, that the rhythmic signals can be well recapitulated across different studies and/or different platforms (Figure 1, Figure 4A). Meta-analysis and multi-omics data integration remain an open-ended question in circadian rhythm detection [42]. In addition, transfer learning has been applied to multiple genomic research domains in genomics [43] – to borrow information and to transfer knowledge from existing data deposited in public repositories remain one of the future directions. Similarly, across different methods, an ensemble framework, as implemented by MetaCycle, can potentially boost performance. However, as we have pointed out earlier, the instability issue needs to be addressed, especially when multiple drastically distinct results are to be integrated.

To our best knowledge, all existing studies for circadian rhythm detection resort to bulk-tissue omics data, which characterize an averaged profile across different cell types in a tissue. The inherent heterogeneity can bias the analysis with reduced power and/or inflated FDR. Single-cell sequencing circumvents the averaging artifacts associated with traditional bulk population data and has seen rapid technological developments over the past few years. To assess the feasibility of single-cell circadian rhythm detection, we *in silico* generated single-cell RNA sequencing profiles by downsampling bulk RNA-seq read counts. Gold-standard circadian and noncircadian genes were used to calculate the associated AUC values (Supplementary Table 7). All methods suffer from low sequencing depth – a characteristic of the single-cell data. With the decreasing cost and the increasing popularity of single-cell omics techniques, to profile circadian rhythmicity at the cellular level and to disentangle within tissue heterogeneity with regard to biological rhythm can be of great impact.

403

404 **MATERIALS AND METHODS**

405 **Empirical transcriptomic datasets**

406 Three datasets under the dark-dark experimental design including Hughes 2009 [18],
407 Hughes 2012 [19], and Zhang 2014 [20] were downloaded from GEO, and all used
408 microarrays to profile gene expressions (Table 2A). Additionally, we obtained four
409 datasets under the light-dark experimental design from the different sequencing platforms,
410 including Nascent-sequencing (Nascent-seq) [22], RNA-sequencing (RNA-seq) [22],
411 Global Run-On sequencing (GRO-seq) [23], and eXcision Repair-sequencing (XR-seq)
412 [24] (Table 2B). Nascent-seq sequence transcribed RNAs, obtained from the nuclei
413 without formation of the 3' end [44]. GRO-seq measures nascent RNAs by mapping,
414 characterizing, and evaluating transcriptionally engaged polymerase [45]. GRO-seq and
415 Nascent-seq differ from traditional RNA-seq, in which the reads map to predominantly
416 introns, while RNA-seq mainly assays exons [44]. XR-seq profiles DNA excision repair
417 on the genome-wide scale with single-nucleotide resolution [46]. Here, we focus on XR-
418 seq data from the transcribed strand only – it has been shown that the transcription-
419 coupled repair from the transcribed strand is positively correlated with expression [47].

420 For quality control, we removed genes that had constant gene expression
421 measurements in all datasets and further removed genes with more than half zero gene
422 expression values in the light-dark datasets. In cases where multiple probes got mapped
423 to the same RefSeq loci, we averaged the gene expression of the probes using the limma
424 package [48], available in Bioconductor. For data normalization, robust multi-array
425 average (RMA) [49] and genechip RMA (GC-RMA) [50] were used to normalize the array
426 data; transcript per million (TPM) and reads per kilobase per million reads (RPKM) [51]
427 were used to normalize the transcriptomic sequencing data. We scaled the normalized
428 data within each gene to make them compatible for visualization only, as shown in Figure
429 1 and Figure 4A.

430

431 **Empirical proteomic dataset**

432 A proteomic dataset of *Mus musculus* liver tissues from Robles et. al [27] was adopted to
433 detect oscillatory proteins. Mouse liver samples were collected from a total of 64 mice

434 that were released into constant darkness for one day after being entrained to a 12-12
435 hour light-dark schedule for 10 days. Four mice were sacrificed every 3 hours for 2 days.
436 Then, in vivo Stable Isotope Labeling by Amino acids in Cell culture (SILAC) [52, 53] in
437 combination with mass spectrometry was performed to profile the proteome. For each
438 time point, equal amount of protein liver extracts from the four mice were mixed together
439 with equal amount of protein lysates, collected in anti-phase, from the liver samples of
440 two SILAC mice. The pooled protein extracts were measured with Orbitrap mass
441 spectrometer. The protein abundance was calculated by taking the ratio of the signal for
442 the mice and the signal for the heavy SILAC mix. After assessing quantification values, a
443 total of 3,132 proteins remained for downstream circadian rhythm analysis.
444
445 **Downsampled RNA-seq dataset**
446 We generated several downsampled RNA-seq datasets from the original RNA-seq
447 dataset under the light-dark design to assess the robustness of the various methods to
448 low sequencing depths. We obtained the raw sequencing data from GEO, performed read
449 alignment to the mouse reference genome (mm10) using STAR [54], carried out quality
450 control procedures on the aligned reads, and obtained integer-valued read counts using
451 featureCounts [55]. We then generated downsampled RNA-seq data by multinomial
452 sampling with index 5K, 10K, 50K, 100K, and 500K, and gene-specific probability
453 parameters calculated from the raw data. RPKM was used to normalize the downsampled
454 RNA-seq read counts, followed by circadian rhythm detection.
455
456 **Evaluation metrics**
457 To evaluate the performance of the benchmarked methods, we adopted a list of 104
458 circadian [10] and 113 non-circadian genes [21] in mouse liver as positive and negative
459 controls, respectively. See Supplementary Table 1 for a full list of these gold-standard
460 genes. With these gold-standard genes, we calculated metrics including the precision and
461 recall rates given a p-value or q-value significance threshold (Figure 2A). We further
462 calculated the AUC values of the ROC curves, as joint measures of sensitivity and
463 specificity (Figure 2B).

To assess the reproducibility of each method, we compared the results from the four dark-dark datasets by calculating the number of overlapping genes, as well as the Jaccard and Sorensen index as metrics for similarity (Figure 3). Venn diagrams are used to display the number of overlapping cycling genes identified across different datasets by each method. The Jaccard index measures the pairwise similarities of the significant genes detected between each pair of datasets. Let A_i and A_j be the set of significant genes from dataset i and j. The Jaccard similarity index is defined as

$$J(A_i, A_j) = \frac{|A_i \cap A_j|}{|A_i \cup A_j|}.$$

The Sorensen Index is used to characterize similarity across all datasets [56]:

$$S(A_i, A_j, A_k, \dots) = \frac{T}{T-1}\left(\frac{\sum_{i<j}|A_i \cap A_j| - \sum_{i<j<k}|A_i \cap A_j \cap A_k| + \sum_{i<j<k<l}|A_i \cap A_j \cap A_k \cap A_l| - \cdots}{\sum_i |A_i|}\right)$$

where T is the number of sets compared. Larger number of overlapping genes and larger Jaccard/Sorensen index values indicate higher reproducibility of the methods.

Simulation setup

Each simulated dataset consists of 6,000 circadian and 6,000 non-circadian gene profiles. Stationary circadian profiles with a period of 24 hours are used in each simulation group, as outlined below. Note that when running the methods, we set the period range from 20 to 28 h for all methods except for eJTK_CYCLE and JTK_CYCLE, which either has a fixed period of 24 h or adjusts the period on the fly. The amplitude of the waveforms is sampled from a uniform distribution between 1 and 6; the phase shift is sampled from a uniform distribution between 0 and 24 h; and the noise term is sampled from a standard normal distribution. Flat waveforms are used to generate non-circadian profiles in all simulation groups except for testing against non-stationary waveforms where linear lines are used.

We first aimed to investigate whether higher sampling frequency or longer sampling time-window is more beneficial for each method. In this simulation group, we generated two datasets with different sampling frequencies and sampling time-windows. With six time-points, we generated one dataset at 4 h/1 day and another at 8 h/2 days; with eight time-points, we generated one dataset at 3 h/1 day and another at 6 h/2 days; with 12 time-points, we generated one dataset at 2 h/1 day and another at 4 h/2 days.

Next, we assessed whether the inclusion of replicates can offset the effect of low sampling frequency in methods' ability of detecting oscillations. Replicates are defined as multiple measurements taken at the same time-point. Specifically, we generated two datasets consisting of the same number of observations, with or without replicates: one at 4 h/1 day X1 and the other at 8 h/1 day X2. The sampling design of the other two pairs of datasets are 3 h/1 day X1 v.s. 6 h/1 day X2, and 2 h/1 day X1 v.s. 4 h/1 day X2.

Since biological rhythms can take on various waveforms, we generated three types of waveforms via simulation: stationary, non-stationary, and asymmetric curves. Supplementary Table 4 includes models that we adopted *in silico* to generate the corresponding waveforms. Specifically, the stationary waveforms include cosine, cosine 2, and cosine peak curves; the non-stationary waveforms include cosine damp, trend exponential, and trend linear curves; the asymmetric subgroup consists of only the saw-tooth waveform. We assessed the performance of the methods in identifying each category of the circadian waveforms.

The next three groups of simulations aimed to determine which methods are more robust to different levels of signal-to-noise ratios, uneven samplings, and missing values. Specifically, we generated four datasets with SNRs of 0.5, 1, 2, and 3. Signal-to-noise ratio is defined by taking the ratio of the empirical variance of cosine function and the variance of the noise, the latter of which is fixed at one. Uneven samplings are defined as designs whose time-points are not equally spaced. To investigate the effect of uneven samplings on performance, we generated datasets with one, two, or four uneven samplings. With six time-points, datasets with four uneven samplings cannot be generated as it would only have two time-points. For missing data, we generated three levels of missing data (1%, 5%, and 10%) at three fixed, randomly selected time-points.

Lastly, we generated three datasets with sampling patterns of 1 h/2 days, 2 h/2 days, and 4 h/2 days to compute the execution times for each method. We seek to identify the differences in computational efficiency among the methods and to explore the effect of increasing sampling resolution on the execution time. Each dataset consists of a total of 6,000 genes. All execution times are reported by running on a Macbook Pro (15-inch, 2019) with 2.3 GHz 8-Core Intel Core i9 and 16 GB memory.

DATA AND SOFTWARE AVAILABILITY

MetaCycle is an open-source R package available at https://github.com/gangwug/MetaCycle and is also used for individual analysis for LS, JTK_CYCLE, and ARSER. RAIN is a Bioconductor R package available at https://bioconductor.org/packages/rain/. eJTK_CYCLE was downloaded from https://github.com/alanlhutchison/empirical-JTK_CYCLE-with-asymmetry. BIO_CYCLE was downloaded from http://circadiomics.igb.uci.edu/BIO_CYCLE. All empirical datasets were downloaded from the NCBI Gene Expression Omnibus (https://www.ncbi.nlm.nih.gov/geo/). The accession numbers for dark-dark datasets are GSE11923, GSE30411, and GSE54652, respectively. The accession numbers for light-dark datasets are GSE59486, GSE36872, GSE36871 and GSE109938, respectively. The proteomic dataset was downloaded from the BioStudies database with accession number S-EPMC3879213.

ACKNOWLEDGEMENTS

This work was supported by NIH Grants R35 GM118102 (to A.S.), R01 ES027255 (to A.S.), P01 CA142538 (to Y.J.), UL1 TR002489 (to Y.J.), and a pilot award from the UNC Computational Medicine Program (to Y.J.). We thank the Sancar Lab members and Dr. John Hogenesch for helpful discussions and feedback.

REFERENCES

1. Li J, Grant GR, Hogenesch JB, Hughes ME: **Considerations for RNA-seq analysis of circadian rhythms.** *Methods Enzymol* 2015, **551:**349-367.

2. Panda S, Antoch MP, Miller BH, Su AI, Schook AB, Straume M, Schultz PG, Kay SA, Takahashi JS, Hogenesch JB: **Coordinated transcription of key pathways in the mouse by the circadian clock.** *Cell* 2002, **109:**307-320.

3. Hughes ME, Hogenesch JB, Kornacker K: **JTK_CYCLE: an efficient nonparametric algorithm for detecting rhythmic components in genome-scale data sets.** *J Biol Rhythms* 2010, **25:**372-380.

4. Asher G, Sassone-Corsi P: **Time for food: the intimate interplay between nutrition, metabolism, and the circadian clock.** *Cell* 2015, **161:**84-92.

5. Partch CL, Green CB, Takahashi JS: **Molecular architecture of the mammalian circadian clock.** *Trends Cell Biol* 2014, **24:**90-99.

558 6. Roenneberg T, Merrow M: **The Circadian Clock and Human Health.** *Curr Biol* 2016,
559 **26:**R432-443.

560 7. Levi F, Schibler U: **Circadian rhythms: mechanisms and therapeutic implications.** *Annu*
561 *Rev Pharmacol Toxicol* 2007, **47:**593-628.

562 8. Glynn EF, Chen J, Mushegian AR: **Detecting periodic patterns in unevenly spaced gene**
563 **expression time series using Lomb-Scargle periodograms.** *Bioinformatics* 2006, **22:**310-
564 316.

565 9. Wijnen H, Naef F, Young MW: **Molecular and statistical tools for circadian transcript**
566 **profiling.** *Methods Enzymol* 2005, **393:**341-365.

567 10. Wu G, Zhu J, Yu J, Zhou L, Huang JZ, Zhang Z: **Evaluation of five methods for genome-**
568 **wide circadian gene identification.** *J Biol Rhythms* 2014, **29:**231-242.

569 11. Yang R, Su Z: **Analyzing circadian expression data by harmonic regression based on**
570 **autoregressive spectral estimation.** *Bioinformatics* 2010, **26:**i168-174.

571 12. Thaben PF, Westermark PO: **Detecting rhythms in time series with RAIN.** *J Biol Rhythms*
572 2014, **29:**391-400.

573 13. Hutchison AL, Maienschein-Cline M, Chiang AH, Tabei SM, Gudjonson H, Bahroos N,
574 Allada R, Dinner AR: **Improved statistical methods enable greater sensitivity in rhythm**
575 **detection for genome-wide data.** *PLoS Comput Biol* 2015, **11:**e1004094.

576 14. Wu G, Anafi RC, Hughes ME, Kornacker K, Hogenesch JB: **MetaCycle: an integrated R**
577 **package to evaluate periodicity in large scale data.** *Bioinformatics* 2016, **32:**3351-3353.

578 15. Agostinelli F, Ceglia N, Shahbaba B, Sassone-Corsi P, Baldi P: **What time is it? Deep**
579 **learning approaches for circadian rhythms.** *Bioinformatics* 2016, **32:**i8-i17.

580 16. Deckard A, Anafi RC, Hogenesch JB, Haase SB, Harer J: **Design and analysis of large-scale**
581 **biological rhythm studies: a comparison of algorithms for detecting periodic signals in**
582 **biological data.** *Bioinformatics* 2013, **29:**3174-3180.

583 17. Hughes ME, Abruzzi KC, Allada R, Anafi R, Arpat AB, Asher G, Baldi P, de Bekker C, Bell-
584 Pedersen D, Blau J, et al: **Guidelines for Genome-Scale Analysis of Biological Rhythms.** *J*
585 *Biol Rhythms* 2017, **32:**380-393.

586 18. Hughes ME, DiTacchio L, Hayes KR, Vollmers C, Pulivarthy S, Baggs JE, Panda S, Hogenesch
587 JB: **Harmonics of circadian gene transcription in mammals.** *PLoS Genet* 2009, **5:**e1000442.

588 19. Hughes ME, Hong HK, Chong JL, Indacochea AA, Lee SS, Han M, Takahashi JS, Hogenesch
589 JB: **Brain-specific rescue of Clock reveals system-driven transcriptional rhythms in**
590 **peripheral tissue.** *PLoS Genet* 2012, **8:**e1002835.

591 20. Zhang R, Lahens NF, Ballance HI, Hughes ME, Hogenesch JB: **A circadian gene expression**
592 **atlas in mammals: implications for biology and medicine.** *Proc Natl Acad Sci U S A* 2014,
593 **111:**16219-16224.

594 21. Wu G, Zhu J, He F, Wang W, Hu S, Yu J: **Gene and genome parameters of mammalian**
595 **liver circadian genes (LCGs).** *PLoS One* 2012, **7:**e46961.

596 22. Menet JS, Rodriguez J, Abruzzi KC, Rosbash M: **Nascent-Seq reveals novel features of**
597 **mouse circadian transcriptional regulation.** *Elife* 2012, **1:**e00011.

598 23. Fang B, Everett LJ, Jager J, Briggs E, Armour SM, Feng D, Roy A, Gerhart-Hines Z, Sun Z,
599 Lazar MA: **Circadian enhancers coordinate multiple phases of rhythmic gene**
600 **transcription in vivo.** *Cell* 2014, **159:**1140-1152.

601 24. Yang Y, Adebali O, Wu G, Selby CP, Chiou YY, Rashid N, Hu J, Hogenesch JB, Sancar A:
602 **Cisplatin-DNA adduct repair of transcribed genes is controlled by two circadian**
603 **programs in mouse tissues.** *Proc Natl Acad Sci U S A* 2018, **115:**E4777-E4785.

604 25. Huang da W, Sherman BT, Lempicki RA: **Systematic and integrative analysis of large gene**
605 **lists using DAVID bioinformatics resources.** *Nat Protoc* 2009, **4:**44-57.

606 26. Huang da W, Sherman BT, Lempicki RA: **Bioinformatics enrichment tools: paths toward**
607 **the comprehensive functional analysis of large gene lists.** *Nucleic Acids Res* 2009, **37:**1-
608 13.

609 27. Robles MS, Cox J, Mann M: **In-vivo quantitative proteomics reveals a key contribution**
610 **of post-transcriptional mechanisms to the circadian regulation of liver metabolism.**
611 *PLoS Genet* 2014, **10:**e1004047.

612 28. Storey JD, Tibshirani R: **Statistical significance for genomewide studies.** *Proc Natl Acad*
613 *Sci U S A* 2003, **100:**9440-9445.

614 29. Li J, Ji L: **Adjusting multiple testing in multilocus analyses using the eigenvalues of a**
615 **correlation matrix.** *Heredity (Edinb)* 2005, **95:**221-227.

616 30. Conneely KN, Boehnke M: **So many correlated tests, so little time! Rapid adjustment of**
617 **P values for multiple correlated tests.** *Am J Hum Genet* 2007, **81:**1158-1168.

618 31. Schwartzman A, Lin X: **The effect of correlation in false discovery rate estimation.**
619 *Biometrika* 2011, **98:**199-214.

620 32. Hutchison AL, Dinner AR: **Correcting for Dependent P-values in Rhythm Detection.**
621 *BioRxiv* 2017.

622 33. Hutchison AL, Allada R, Dinner AR: **Bootstrapping and Empirical Bayes Methods Improve**
623 **Rhythm Detection in Sparsely Sampled Data.** *J Biol Rhythms* 2018, **33:**339-349.

624 34. Ceglia N, Liu Y, Chen S, Agostinelli F, Eckel-Mahan K, Sassone-Corsi P, Baldi P: **CircadiOmics:**
625 **circadian omic web portal.** *Nucleic Acids Res* 2018, **46:**W157-W162.

626 35. Masri S, Patel VR, Eckel-Mahan KL, Peleg S, Forne I, Ladurner AG, Baldi P, Imhof A,
627 Sassone-Corsi P: **Circadian acetylome reveals regulation of mitochondrial metabolic**
628 **pathways.** *Proc Natl Acad Sci U S A* 2013, **110:**3339-3344.

629 36. Mauvoisin D, Atger F, Dayon L, Nunez Galindo A, Wang J, Martin E, Da Silva L, Montoliu I,
630 Collino S, Martin FP, et al: **Circadian and Feeding Rhythms Orchestrate the Diurnal Liver**
631 **Acetylome.** *Cell Rep* 2017, **20:**1729-1743.

632 37. Dallmann R, Viola AU, Tarokh L, Cajochen C, Brown SA: **The human circadian metabolome.**
633 *Proc Natl Acad Sci U S A* 2012, **109:**2625-2629.

634 38. Feng D, Lazar MA: **Clocks, metabolism, and the epigenome.** *Mol Cell* 2012, **47:**158-167.

635 39. Jiang Y, Wang R, Urrutia E, Anastopoulos IN, Nathanson KL, Zhang NR: **CODEX2: full-**
636 **spectrum copy number variation detection by high-throughput DNA sequencing.**
637 *Genome Biol* 2018, **19:**202.

638 40. Singer JM, Fu DY, Hughey JJ: **Simphony: simulating large-scale, rhythmic data.** *PeerJ* 2019,
639 **7:**e6985.

640 41. Li X, Shi L, Zhang K, Wei W, Liu Q, Mao F, Li J, Cai W, Chen H, Teng H, et al: **CirGRDB: a**
641 **database for the genome-wide deciphering circadian genes and regulators.** *Nucleic Acids*
642 *Res* 2018, **46:**D64-D70.

643 42. Patel VR, Eckel-Mahan K, Sassone-Corsi P, Baldi P: **CircadiOmics: integrating circadian**
644 **genomics, transcriptomics, proteomics and metabolomics.** *Nat Methods* 2012, **9:**772-
645 773.

646 43. Eraslan G, Avsec Z, Gagneur J, Theis FJ: **Deep learning: new computational modelling**
647 **techniques for genomics.** *Nat Rev Genet* 2019, **20:**389-403.

648 44. Trott AJ, Menet JS: **Regulation of circadian clock transcriptional output by CLOCK:BMAL1.**
649 *PLoS Genet* 2018, **14:**e1007156.

650 45. Core LJ, Waterfall JJ, Lis JT: **Nascent RNA sequencing reveals widespread pausing and**
651 **divergent initiation at human promoters.** *Science* 2008, **322:**1845-1848.

652 46. Hu J, Adar S, Selby CP, Lieb JD, Sancar A: **Genome-wide analysis of human global and**
653 **transcription-coupled excision repair of UV damage at single-nucleotide resolution.**
654 *Genes Dev* 2015, **29:**948-960.

655 47. Yimit A, Adebali O, Sancar A, Jiang Y: **Differential damage and repair of DNA-adducts**
656 **induced by anti-cancer drug cisplatin across mouse organs.** *Nat Commun* 2019, **10:**309.

657 48. Ritchie ME, Phipson B, Wu D, Hu Y, Law CW, Shi W, Smyth GK: **limma powers differential**
658 **expression analyses for RNA-sequencing and microarray studies.** *Nucleic Acids Res* 2015,
659 **43:**e47.

660 49. Irizarry RA, Hobbs B, Collin F, Beazer-Barclay YD, Antonellis KJ, Scherf U, Speed TP:
661 **Exploration, normalization, and summaries of high density oligonucleotide array probe**
662 **level data.** *Biostatistics* 2003, **4:**249-264.

663 50. Wu Z, Irizarry RA, Gentleman R, Martinez-Murillo F, Spencer F: **A Model-Based**
664 **Background Adjustment for Oligonucleotide Expression Arrays.** *Journal of the American*
665 *Statistical Association* 2004, **99:**909-917.

666 51. Conesa A, Madrigal P, Tarazona S, Gomez-Cabrero D, Cervera A, McPherson A, Szczesniak
667 MW, Gaffney DJ, Elo LL, Zhang X, Mortazavi A: **A survey of best practices for RNA-seq**
668 **data analysis.** *Genome Biol* 2016, **17:**13.

669 52. Geiger T, Cox J, Ostasiewicz P, Wisniewski JR, Mann M: **Super-SILAC mix for quantitative**
670 **proteomics of human tumor tissue.** *Nat Methods* 2010, **7:**383-385.

671 53. Gouw JW, Krijgsveld J, Heck AJ: **Quantitative proteomics by metabolic labeling of model**
672 **organisms.** *Mol Cell Proteomics* 2010, **9:**11-24.

673 54. Dobin A, Davis CA, Schlesinger F, Drenkow J, Zaleski C, Jha S, Batut P, Chaisson M, Gingeras
674 TR: **STAR: ultrafast universal RNA-seq aligner.** *Bioinformatics* 2013, **29:**15-21.

675 55. Liao Y, Smyth GK, Shi W: **featureCounts: an efficient general purpose program for**
676 **assigning sequence reads to genomic features.** *Bioinformatics* 2014, **30:**923-930.

677 56. Diserud OH, Odegaard F: **A multiple-site similarity measure.** *Biol Lett* 2007, **3:**20-22.

678

679 **FIGURE & TABLE LEGENDS**

680 **Figure 1. Examples of circadian and non-circadian benchmark gene expressions**
681 **among three datasets with dark-dark experimental design.** Scaled gene expressions
682 from selected (A) circadian genes including *Clock*, *Cry1*, *Npas2*, and *Per1* and (B) non-
683 circadian genes including *Utp6*, *Mtf1*, *Cln3*, *Abcd4*.

684

685 **Figure 2. Evaluation of seven methods by precision, recall rates and ROC curves.**
686 (A) A p-value threshold of 0.000005 (Bonferroni threshold), 0.00005, 0.0005, and a q-
687 value threshold of 0.05 (FDR threshold) are adopted for each of the seven methods
688 applied to the four dark-dark empirical datasets. A more relaxed threshold results in a
689 higher recall rate, with FDR being the most sensitive, yet this also leads to a higher
690 number of false positives with a lower precision rate. (B) ROC curves and AUC values
691 using gold-standard circadian and non-circadian genes. Each method is evaluated across
692 four dark-dark empirical datasets. Sensitivity and specificity are calculated using the
693 nominal p-values by each method with varying threshold. BIO_CYCLE returns the highest
694 AUC.

695

696 **Figure 3. Evaluation of method reproducibility.** (A) Venn diagrams display the number
697 of cyclic genes that are significant by each method among the four dark-dark datasets.
698 (B) Jaccard index and the Sorensen index are used as metrics for reproducibility for each
699 method across the four datasets with the same experimental design.

700

701 **Figure 4. Circadian rhythm detection under light-dark experimental design by GRO-**
702 **seq, Nascent-seq, RNA-seq, and XR-seq.** (A) Gene-specific measurements of nascent

703 RNA, RNA, and transcription-coupled repair of four circadian benchmark genes, *Clock*,
704 *Npas2*, *Cry1*, and *Per1* by four different sequencing platforms. The solid and dotted lines
705 are used for the first and second replicates respectively. (B) Beehive plots of negative log
706 p-values of base 10 of circadian genes as positive controls. The number of significant
707 genes detected by each method with an FDR threshold of 0.05 are shown in parenthesis.
708 The asterisks denote significant GO enrichments of circadian rhythm pathway. The
709 nominal p-values by JTK_CYCLE, MetaCycle, and BIO_CYCLE are the most significant,
710 while LS and RAIN tend to be underpowered. ARS is not included in the analysis because
711 it cannot be applied to datasets with replicates.
712
713 **Figure 5. Performance assessment via simulation studies.** Seven circadian rhythm
714 detection methods are evaluated under different experimental designs to explore how
715 sampling patterns, replicates, waveforms, signal-to-noise ratios (SNRs), uneven
716 samplings, and missing values affect performance. Simulations under each design are
717 carried out with different sampling frequencies: (A) 4 h/1 day, (B) 3 h/1 day, and (C) 2 h/1
718 day. AUC values calculated from ground truths are used as metrics.
719
720 **Figure 6. Existing methods return non-uniformly distributed p-values under the null,**
721 **partially due to non-independent testing due to gene-gene correlations.** (A) Gene
722 expression values for the benchmark circadian gene *Cry1* before and after random
723 permutations of the time labels. (B) Heatmaps of pairwise correlation coefficients among
724 the top 200 highly variable genes from the Hughes 2009 dataset. The top illustrates the
725 gene-gene correlation coefficients calculated from raw data input, and the bottom shows
726 the gene-gene correlations after permutation. (C) The distributions of nominal p-values
727 for each method when applied to the dataset before and after permutation. Gene-gene
728 correlations, which are accounted for by eJTK_CYCLE, partially lead to the systematic
729 deviations from the null distributions. The hypothesis testing by LS, JTK_CYCLE, RAIN,
730 and MetaCycle are overly conservative, while ARSER's and BIO_CYCLE's testing
731 procedures are biased with an overabundance of p-values around 0.3 and 0.1,
732 respectively, under the null.
733

734 **Table 1. Summary of seven existing methods for circadian rhythm detection.** [a]
735 BIO_CYCLE can be applied to datasets with missing values only if there are replicates
736 and the missingness only pertains to part of the replicates.
737
738 **Table 2. High-throughput mouse liver datasets adopted for circadian rhythm**
739 **detection.** (A) Dark-dark experimental design. (B) Light-dark experimental design.
740
741 **Table 3. Pros and cons of circadian rhythm detection methods.**
742
743 **SUPPLEMENTARY FIGURE & TABLE LEGENDS**
744 **Supplementary Table 1. Circadian and non-circadian genes in *Mus muculus* liver**
745 **as gold standard.** The 104 circadian gene list is extracted from Supplementary Table 4
746 in Wu et al. Wu G, Zhu J, Yu J, Zhou L, Huang JZ and Zhang Z [10] and the 113 non-
747 circadian gene list is obtained from Supplementary Table 2 in Wu et al. Wu G, Zhu J, He
748 F, Wang W, Hu S and Yu J [21].
749
750 **Supplementary Table 2. Pathway enrichment analysis of significantly cyclic genes**
751 **from the light-dark datasets.** Functional annotations (KEGG pathway mapping) of the
752 significant genes (q-values ≤ 0.05) are carried out using the the DAVID Bioinformatics
753 Resources (https://david.ncifcrf.gov/). The list only contains significantly enriched
754 pathways with a 0.05 cutoff of the p-values adjusted by Benjamini Hochberg.
755
756 **Supplementary Table 3. Pathway enrichment analysis of significantly cyclic**
757 **proteins.** Functional annotations (KEGG pathway mapping) of the significant proteins (q-
758 values ≤ 0.05) are carried out using the the DAVID Bioinformatics Resources
759 (https://david.ncifcrf.gov/). The list only contains significantly enriched pathways with a
760 0.05 cutoff of the p-values adjusted by Benjamini Hochberg. KEGG metabolic pathways
761 were enriched by all three methods.
762
763 **Supplementary Table 4. *In silico* generated periodic v.s. non-periodic gene profiles.**
764 Three types of periodic waveforms are included: stationary, non-stationary, and

765 asymmetric. The stationary and non-stationary subgroups consist of three forms of cosine
766 curves. The asymmetric subgroup consists of a saw-tooth waveform. Flat or linear lines
767 are adopted to generate non-periodic waveforms. The waveforms shown are constructed
768 without noise. 'Amp', 'pha', and 'per' represent amplitude, phase and period, respectively.
769
770 **Supplementary Table 5. Details of simulation setup and parameters used to *in silico***
771 **generate periodic and non-periodic profiles.** Each simulation run consists of 6,000
772 periodic and 6,000 non-periodic gene profiles. All simulated waveforms have a period
773 length of 24, a phase shift that is uniformly distributed between 0 and 24, and a noise
774 term with standard normal distribution. The amplitude is uniformly distributed between 1
775 and 6 for all groups except when testing for different signal-to-noise ratios (SNRs), which
776 we define as the ratios of the empirical variances of the cosine function and the variances
777 of the noise. Non-periodic profiles are sampled from a flat/linear function. "X 1" indicates
778 no replicate and "X 2" indicates two replicates.
779
780 **Supplementary Table 6. Evaluation of computational efficiency with different**
781 **sampling rates.** Each method is run on a dataset with a total of 6,000 genes. All
782 programs are run on a Macbook Pro (15-inch, 2019) with 2.3 GHz 8-Core Intel Core i9
783 and 16 GB memory. Running time for MetaCycle is the sum of the runing time for LS,
784 ARSER, and JTK_CYCLE. Running time for BIO_CYCLE does not include the time used
785 to fit the deep neural network.
786
787 **Supplementary Table 7. Performance assessment of downsampled RNA-seq data.**
788 AUC values of downsampled RNA-seq datasets with varying sequencing depths were
789 calculated. Existing methods suffer from low sequencing depths. The performance of
790 RAIN exceeds that of all other methods in all sequencing depths with an exception at 5K,
791 due to its large number of significant genes detected in general. BIO_CYCLE consistently
792 ranks the lowest at all but the highest sequencing depth. The performances of LS,
793 JTK_CYCLE, eJTK_CYCLE, and MetaCycle are comparable.
794

795 **Supplementary Figure 1. Circadian rhythm detection of *Mus musculus* liver**
796 **protemoic dataset.** (A) Bar plot of the number of significant proteins detected by each
797 method using an FDR threshold of 0.05. Only methods that are able to handle both
798 replicates and missing values were applied and evaluated. (B) Heatmap of scaled
799 measurements of oscillatory proteins identified by at least two methods. Proteins (rows)
800 are ordered based on their inferred phases.
801
802 **Supplementary Figure 2. Decision tree as user guidance on method selection.** The
803 decision tree has decision rules for sampling resolutions, uneven samplings, replicates,
804 and missing values.

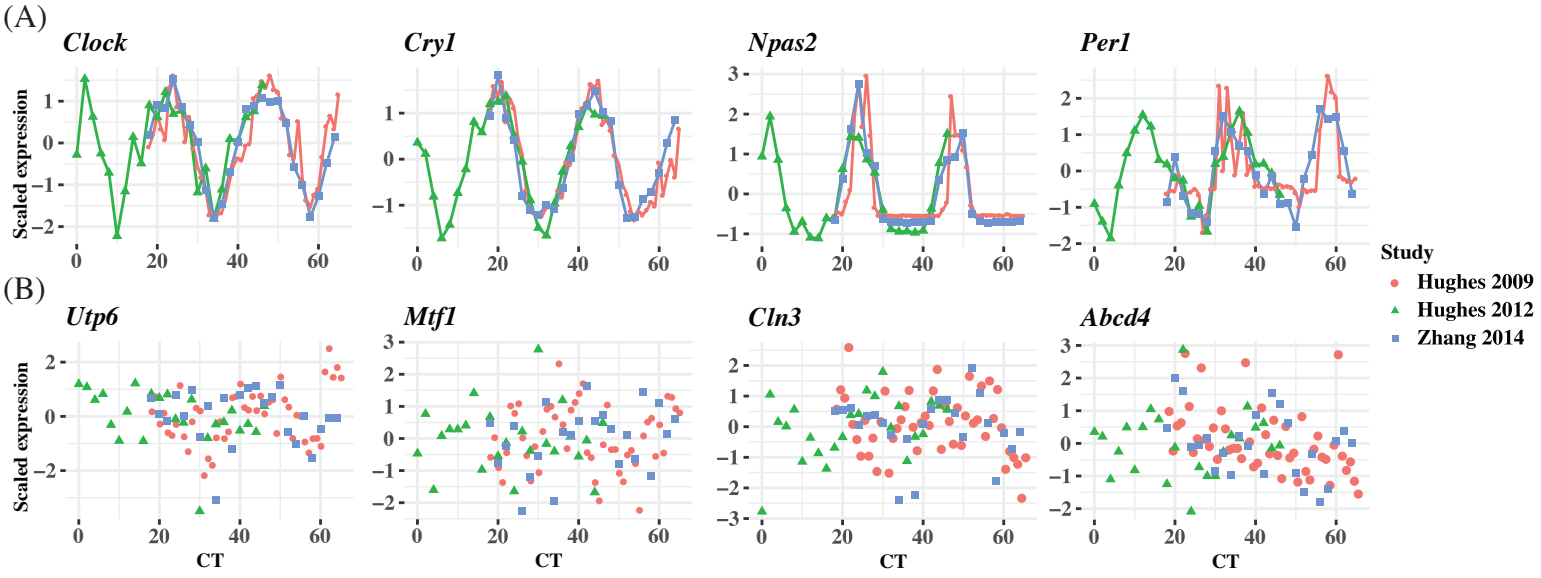
(A)
Clock
Cry1
Npas2
Per1
(B)
Utp6
Mtf1
Cln3
Abcd4
Scaled expression
CT
Study
Hughes 2009
Hughes 2012
Zhang 2014

Figure 1

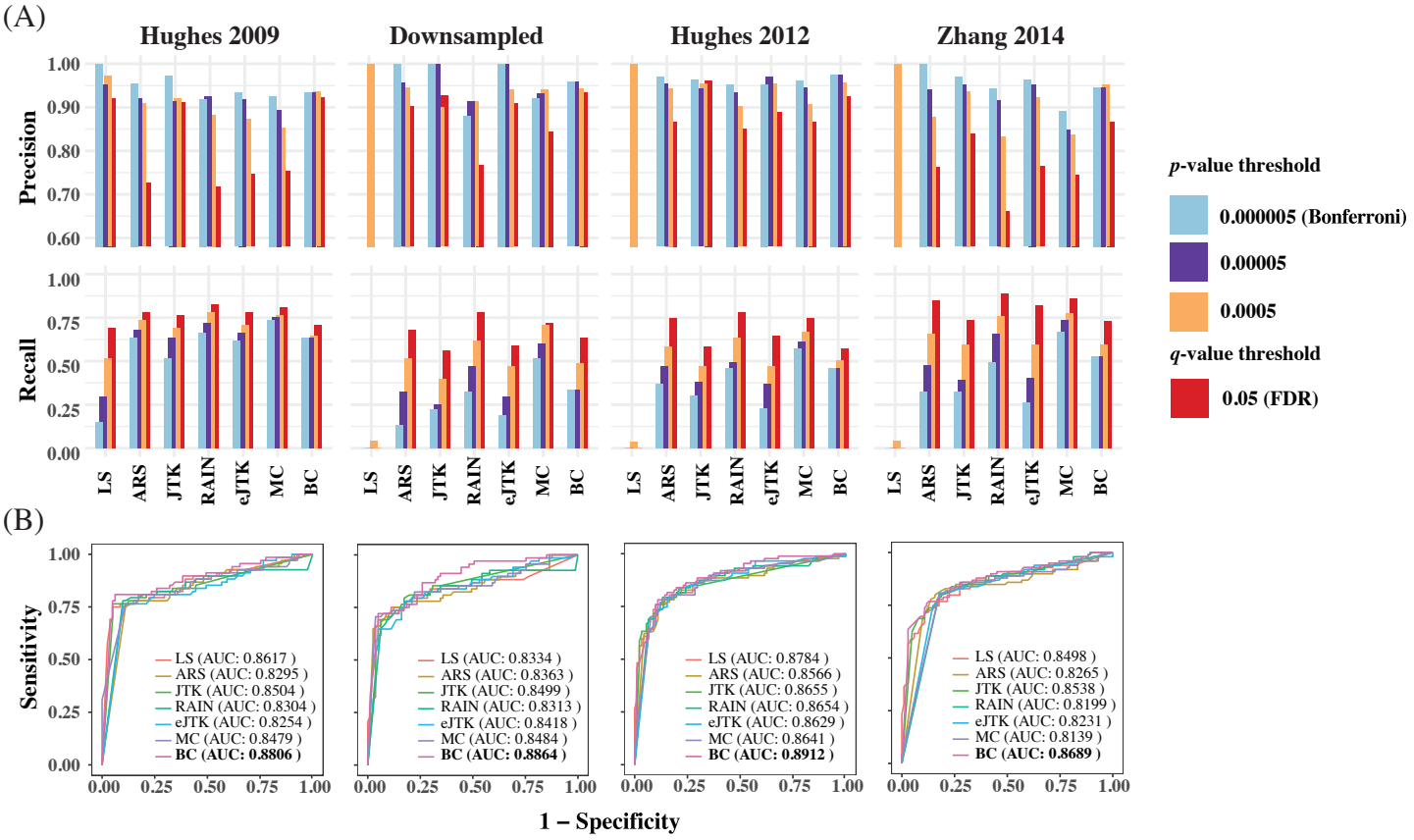
(A)
Hughes 2009
Downsampled
Hughes 2012
Zhang 2014
Precision
Recall
LS
ARS
JTK
RAIN
eJTK
MC
BC
p-value threshold
0.000005 (Bonferroni)
0.00005
0.0005
q-value threshold
0.05 (FDR)
(B)
Sensitivity
1 – Specificity
LS (AUC: 0.8617)
ARS (AUC: 0.8295)
JTK (AUC: 0.8504)
RAIN (AUC: 0.8304)
eJTK (AUC: 0.8254)
MC (AUC: 0.8479)
BC (AUC: 0.8806)
LS (AUC: 0.8334)
ARS (AUC: 0.8363)
JTK (AUC: 0.8499)
RAIN (AUC: 0.8313)
eJTK (AUC: 0.8418)
MC (AUC: 0.8484)
BC (AUC: 0.8864)
LS (AUC: 0.8784)
ARS (AUC: 0.8566)
JTK (AUC: 0.8655)
RAIN (AUC: 0.8654)
eJTK (AUC: 0.8629)
MC (AUC: 0.8641)
BC (AUC: 0.8912)
LS (AUC: 0.8498)
ARS (AUC: 0.8265)
JTK (AUC: 0.8538)
RAIN (AUC: 0.8199)
eJTK (AUC: 0.8231)
MC (AUC: 0.8139)
BC (AUC: 0.8689)

Figure 2

(A)

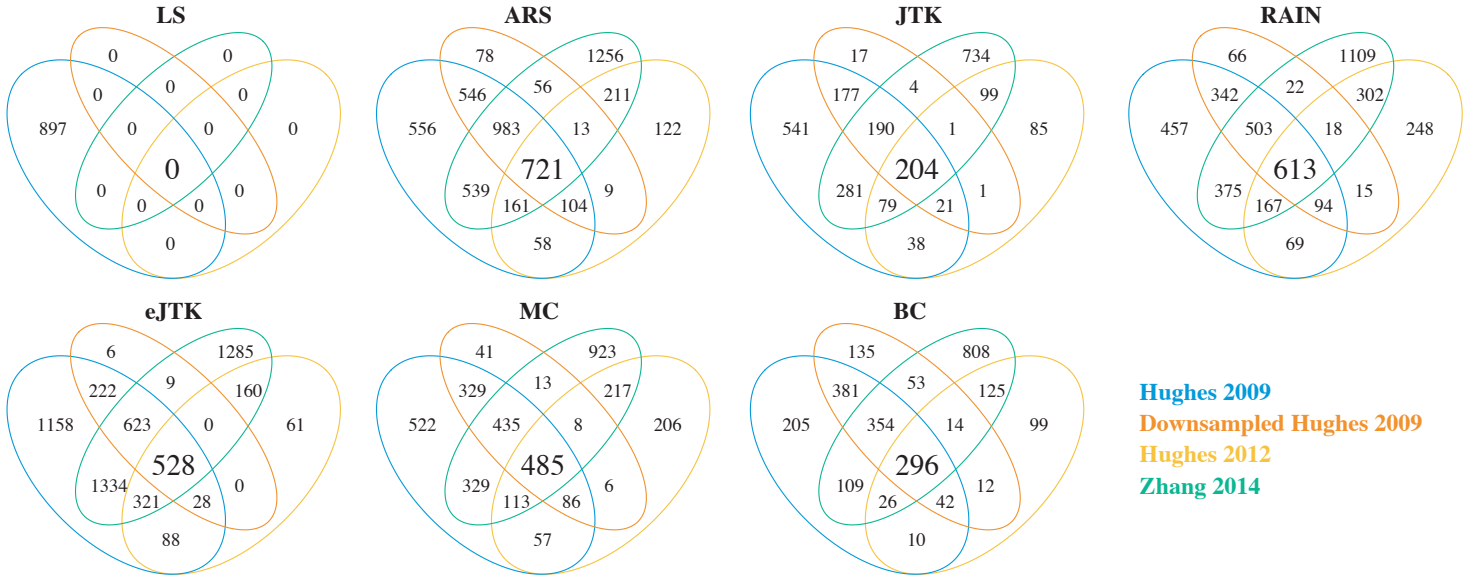

(B)

Hughes 2009	0	0	0
	Down-sampled	NA	NA
		Hughes 2012	NA
			Zhang 2014

LS
Sorensen Index = 0

Hughes 2009	0.6156	0.2595	0.4620
	Down-sampled	0.2766	0.3791
		Hughes 2012	0.2613
			Zhang 2014

ARS
Sorensen Index = 0.7067

Hughes 2009	0.3810	0.1992	0.3183
	Down-sampled	0.2478	0.2207
		Hughes 2012	0.2205
			Zhang 2014

JTK
Sorensen Index = 0.5607

Hughes 2009	0.5662	0.2944	0.4073
	Down-sampled	0.3009	0.3188
		Hughes 2012	0.3112
			Zhang 2014

RAIN
Sorensen Index = 0.6762

Hughes 2009	0.3245	0.2136	0.4875
	Down-sampled	0.2717	0.2569
		Hughes 2012	0.2274
			Zhang 2014

eJTK
Sorensen Index = 0.6379

Hughes 2009	0.5507	0.2653	0.3873
	Down-sampled	0.2931	0.3152
		Hughes 2012	0.2860
			Zhang 2014

MC
Sorensen Index = 0.6595

Hughes 2009	0.6555	0.2236	0.3240
	Down-sampled	0.2353	0.3045
		Hughes 2012	0.2367
			Zhang 2014

BC
Sorensen Index = 0.6381

Figure 3

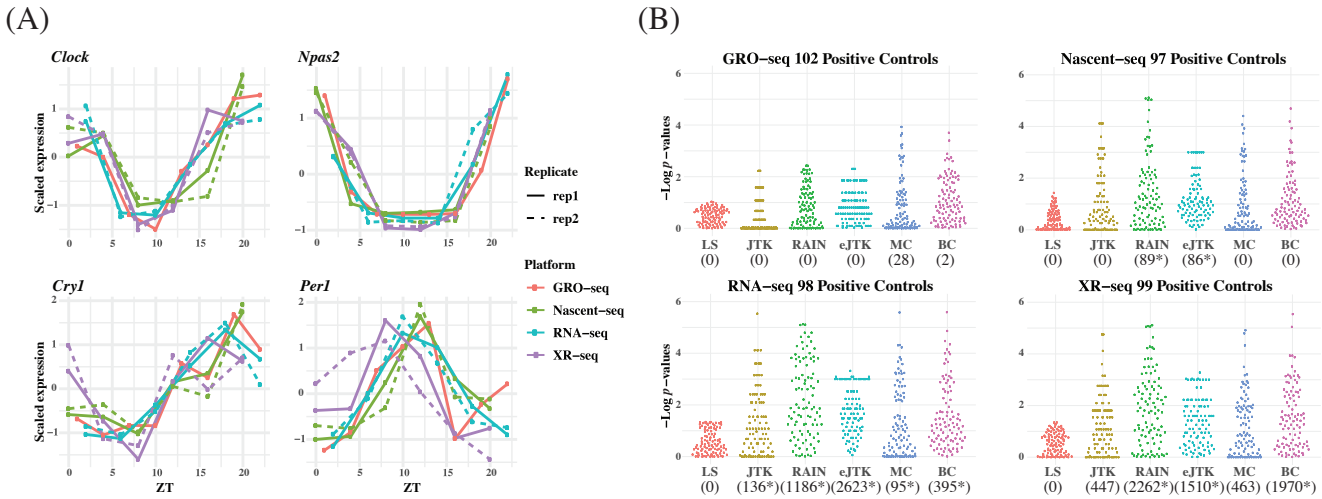
(A)
Clock
Npas2
Cry1
Per1
Scaled expression
ZT
Replicate
rep1
rep2
Platform
GRO−seq
Nascent−seq
RNA−seq
XR−seq
(B)
GRO−seq 102 Positive Controls
Nascent−seq 97 Positive Controls
RNA−seq 98 Positive Controls
XR−seq 99 Positive Controls
−Log p−values
LS (0)
JTK (0)
RAIN (0)
eJTK (0)
MC (28)
BC (2)
LS (0)
JTK (0)
RAIN (89*)
eJTK (86*)
MC (0)
BC (0)
LS (0)
JTK (136*)
RAIN (1186*)
eJTK (2623*)
MC (95*)
BC (395*)
LS (0)
JTK (447)
RAIN (2262*)
eJTK (1510*)
MC (463)
BC (1970*)

Figure 4

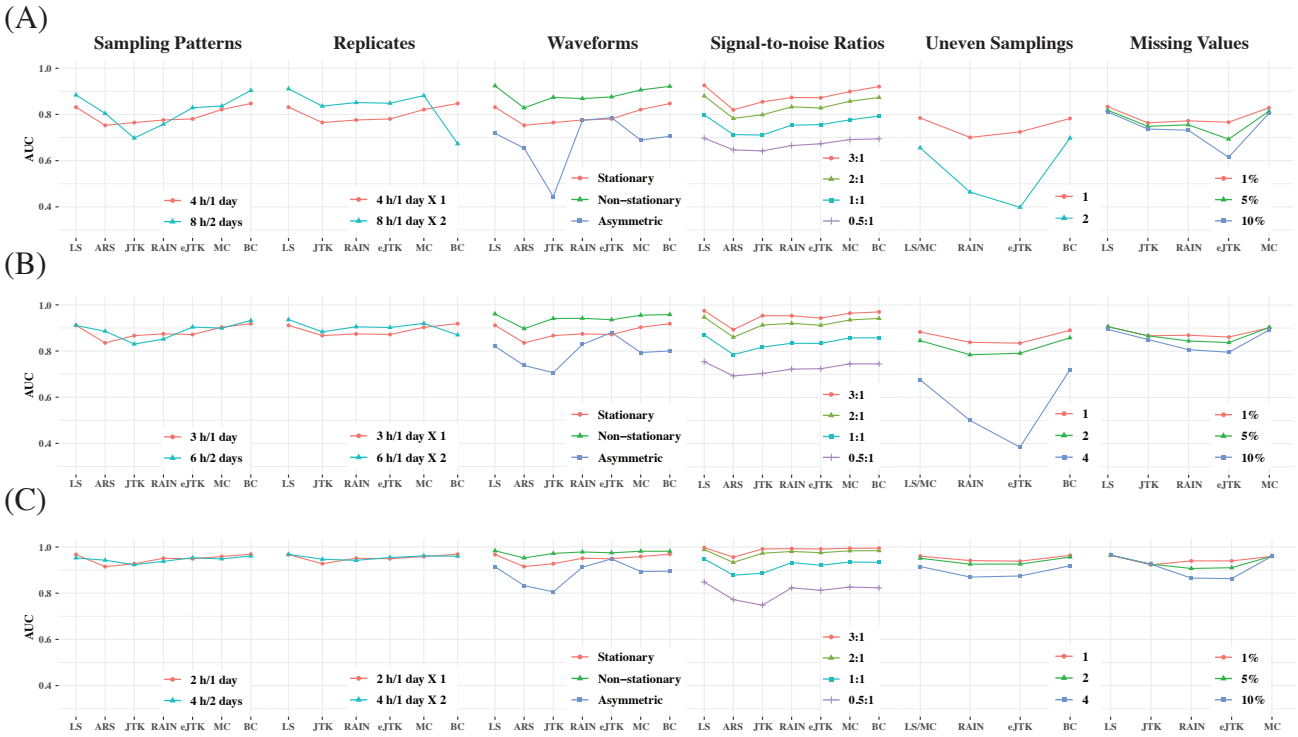
(A)
Sampling Patterns
Replicates
Waveforms
Signal-to-noise Ratios
Uneven Samplings
Missing Values
AUC
1.0
0.8
0.6
0.4
4 h/1 day
8 h/2 days
4 h/1 day X 1
8 h/1 day X 2
Stationary
Non−stationary
Asymmetric
3:1
2:1
1:1
0.5:1
1
2
1%
5%
10%
LS ARS JTK RAIN eJTK MC BC
LS JTK RAIN eJTK MC BC
LS/MC RAIN eJTK BC
(B)
3 h/1 day
6 h/2 days
3 h/1 day X 1
6 h/1 day X 2
4
(C)
2 h/1 day
4 h/2 days
2 h/1 day X 1
4 h/1 day X 2

Figure 5

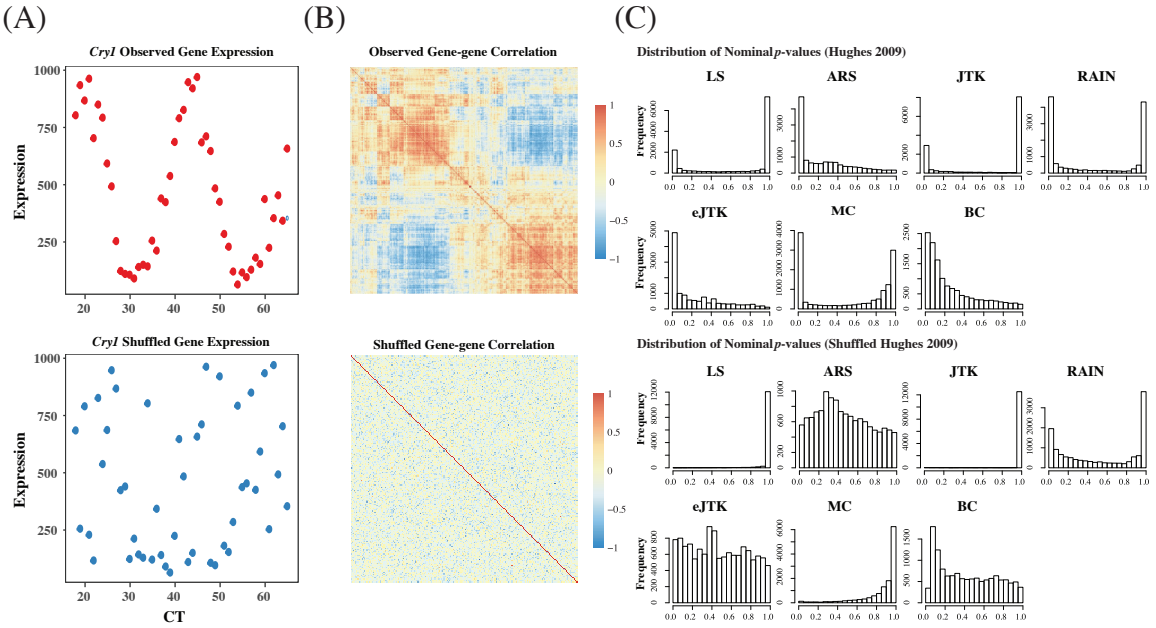
(A)
(B)
(C)
Cry1 Observed Gene Expression
Expression
CT
Observed Gene-gene Correlation
Distribution of Nominal p-values (Hughes 2009)
LS
ARS
JTK
RAIN
eJTK
MC
BC
Frequency
Cry1 Shuffled Gene Expression
Shuffled Gene-gene Correlation
Distribution of Nominal p-values (Shuffled Hughes 2009)

Figure 6

Package	Method Key Words	Method Type	Reference	Availability	Language	Replicates	Missing Values	Uneven Sampling
Lomb-Scargle (LS)	Periodogram	Parametric	*Bioinformatics (2006)*	https://www.iiap.res.in/astrostat/tuts/Lomb-Scargle.html	R	✔	✔	✔
ARSER (ARS)	Harmonic Regression	Parametric	*Bioinformatics (2010)*	http://bioinformatics.cau.edu.cn/ARSER	Python & R	✕	✕	✕
JTK_CYCLE (JTK)	Kendall's Tau	Non-parametric	*J Biol Rhythms (2010)*	https://openwetware.org/wiki/HughesLab:JTK_Cycle	R	✔	✔	✕
RAIN	Asymmetric waveforms	Non-parametric	*J Biol Rhythms (2014)*	http://bioconductor.org/packages/rain	R	✔	✔	✔
eJTK_CYCLE (eJTK)	Empirical *p*-values	Non-parametric	*PLOS Comp. Bio. (2015)*	https://github.com/alanlhutchison/empirical-JTK_CYCLE-with-asymmetry	Python	✔	✔	✔
MetaCycle (MC)	Integration	Parametric	*Bioinformatics (2016)*	https://cran.r-project.org/package=MetaCycle	R	✔	✔	✔
BIO_CYCLE (BC)	Deep Neural Network	Parametric	*Bioinformatics (2016)*	http://circadiomics.igb.uci.edu	R	✔	✔/✕ [a]	✔

Table 1

Design	Name	Reference	Accession Number	Tissue Type	Sequencing Platform	Number of Time Points & Replicates	Number of Genes	Time Points
(A) Dark-Dark	Hughes et al.	*PLOS Genetics (2009)*	GSE11923	Liver	Microarray	48 x 1	13,029	CT18, 19, 20, …, 65
	Hughes et al. (downsampled)	*PLOS Genetics (2009)*	GSE11923	Liver	Microarray	24 x 1	12,506	CT18, 20, 22, …, 64
	Hughes et al.	*PLOS Genetics (2012)*	GSE30411	Liver	Microarray	24 x 1	14,413	CT0, 2, 4, …, 46
	Zhang et al.	*PNAS (2014)*	GSE54652	Liver	Microarray	24 x 1	20,307	CT18, 20, 22, …, 64
(B) Light-Dark	Fang et al.	*Cell (2014)*	GSE59486	Liver	GRO-seq	8 x 1	17,463	ZT1, 4, 7, 10, 13, 16, 19, 22
	Menet et al.	*eLIFE (2012)*	GSE36872	Liver	Nascent-seq	6 x 2	17,917	ZT0, 4, 8, 12, 16, 20
	Menet et al.	*eLIFE (2012)*	GSE36871	Liver	RNA-seq	6 x 2	17,222	ZT2, 6, 10, 14, 18, 22
	Yang et al.	*PNAS (2018)*	GSE109938	Liver	XR-seq (TS)	6 x 2	17,652	ZT0, 4, 8, 12, 16, 20

Table 2

Methods	Pros	Cons
LS	• Effective in handling missing values • Not restricted by input data structure (i.e. can be applied to datasets with replicates, uneven samplings, or missing values)	• Rapid degradation in detectability when applied to datasets with low sampling resolution • U-shaped *p*-values distribution • Sensitive to outliers
ARSER	• High reproducibility	• Cannot handle replicates, uneven samplings, or missing values
JTK_CYCLE	• High precision • Robust to outliers	• Incapable of detecting asymmetric waveforms • U-shaped *p*-values distribution • Sensitive to high level of noise • High false negative rates • Low reproducibility
RAIN	• High recall • Effective in detecting asymmetric waveforms • High reproducibility • Not restricted by input data structure	• High false positive rates • U-shaped *p*-values distribution • Computationally intensive with increasing sampling resolution
eJTK_CYCLE	• Uniform distribution of nominal *p*-values • Most effective in detecting asymmetric waveforms	• Unable to test different periods simultaneously • Inefficient in handling missing values • Sensitive to high level of uneven samplings
MetaCycle	• High recall • Not restricted by input data structure • Offset the disadvantages of one method with the other two among LS, ARSER and JTK_CYCLE • Directly return calling results from three perspective methods and perform ensemble	• *P*-values generated with Fisher's integration require independence assumption
BIO_CYCLE	• Most effective in controlling for false positive rates • Most robust to data with high noise, uneven samplings, and low sampling resolutions. • High precision • High computational efficiency with pre-trained model	• Require extensive time to train the DNN model • Handle missing values only if data have replicates and the missingness only pertains to part of the replicates. • Low reproducibility

Table 3